Int. J. Solids Structures, 1973, Vol. 9, pp. 53 to 68. Pergamon Press. Printed in Great Britain

EXTENSION OF AN INTERFACE FLAW UNDER THE INFLUENCE OF TRANSIENT WAVES

L. M. BROCK

University of Kentucky, Lexington, Kentucky 40506

and

J. D. ACHENBACH

Northwestern University, Evanston, Illinois 60201

Abstract—This paper is concerned with the initiation of debonding at an interface of two elastic solids of different elastic constants and mass densities. The debonding is caused by stress concentrations that are generated when a system of transient horizontally polarized shear waves strikes the tip of an interface flaw. It is assumed that rupture of the adhesive bond is preceded by yielding of the adhesive. It is shown that for a system of step-stress waves the zone of interface yielding initially extends linearly with time. For various values of the parameters defining the materials and the system of waves the speed of the leading edge of the zone of interface yielding is computed. Analytic expressions are presented for the time of rupture and for the interface stress ahead of the yield zone.

1. INTRODUCTION

BODIES consisting of layers of different materials glued, fused or otherwise continuously joined, or simply pressed together, appear in nature as well as in man-made structures. An example in nature is the stratification of the earth. Manufactured laminated media are used frequently for structural applications in engineering.

Generally it is not realistic to assume that the contact between different layers is perfect. Indeed, in geophysical stratifications faults occur at the interfaces, while in manufactured laminates adjoining layers may not be properly adhered, so that the interfaces may contain small and difficult to detect flaws. Under the action of external forces interface flaws give rise to stress concentrations, which may cause a flaw to extend and which thus may form the nucleus of considerable interface failure.

In the analysis of elastodynamic problems it is often found that at certain specific locations in a body the dynamic stresses are higher than the stresses computed from the corresponding problem of static equilibrium. This effect occurs, for example, when a wave is diffracted by a crack. For horizontally polarized shear waves the dynamic overshoot of the stresses near the edge of a crack in a homogeneous material was examined in [1]. It was shown in [1, 2] that in view of the dynamic overshoot of the stress concentrations it is possible that extension of a flaw may or may not occur depending on whether the loads are suddenly or gradually applied.

In this paper we examine the conditions for extension of an interface flaw upon diffraction of a system of transient waves. For incident pulses which show rapid increases of the field variables at the wavefronts, the maximum values of the stresses are reached very shortly after the flaw has been struck. As a consequence we will focus attention on the stress field for small times and in the vicinity of the edge of the flaw. This type of information on the stresses can, however, be obtained by investigating diffraction by an extending semi-infinite flaw at the interface of two half-spaces of distinct solids. To simplify the analysis further we consider the case that the incident waves which propagate along the bonded part of the interface prior to reaching the flaw are horizontally polarized.

As an interface flaw extends, the breaking of the interface bond may be considered as either brittle or ductile fracture. In this paper it is assumed that bond rupture is preceded by plastic deformation of the bond, but not of the adjoining materials. Thus, as the vicinity of the interface flaw is placed in a (dynamic) state of stress, a small region of yielding is assumed to develop at the interface in the vicinity of the edge of the flaw. This zone of yielding grows until the relative displacement between the two materials at the edge of the flaw becomes so great that the yielded bond ruptures and free fracture surface is formed.

2. FORMULATION

Referring to a Cartesian coordinate system x', y', z', we consider two half-spaces of distinct linearly elastic homogeneous isotropic solids whose interface is defined by the plane $y' = 0$, see Fig. 1. For $x' \geq 0$ the half-spaces are in bonded contact, while no bond

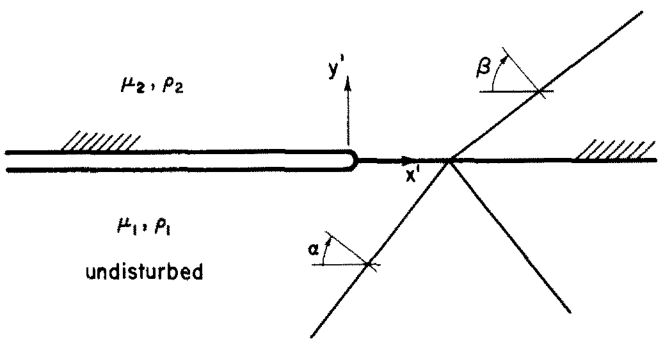

FIG. 1. System of horizontally polarized shear waves approaching an interface flaw.

exists for $x' < 0$. It is assumed that the bonding layer between the half-spaces ($y' = 0$, $x' \geq 0$) has a vanishingly small thickness and is rigid-perfectly plastic in nature.

The material properties and the field variables in region 1, where $y' \leq 0$, and region 2, where $y' \geq 0$, are labeled with the subscripts 1 and 2, respectively. For the two-dimensional problem considered here the propagation of horizontally polarized shear waves in the homogeneous, isotropic, linearly elastic medium of region 1 is governed by the wave equation

$$\nabla^2 w_1 = \frac{1}{c_1^2} \frac{\partial^2 w_1}{\partial t^2}, \tag{2.1}$$

where $w_1(x', y', t)$ is the displacement in the z'-direction, ∇^2 is the two-dimensional Laplacian with respect to the coordinates x' and y', and c_1 is the velocity of shear waves,

$$c_1 = (\mu_1/\rho_1)^{\frac{1}{2}}. \tag{2.2}$$

In (2.2), μ_1 and ρ_1 are the shear modulus and mass density, respectively. The shear stresses in region 1 are

$$(\tau_{y'z'})_1 = \mu_1 \frac{\partial w_1}{\partial y'}, \qquad (\tau_{x'z'})_1 = \mu_1 \frac{\partial w_1}{\partial x'}. \tag{2.3a, b}$$

A set of equations analogous to (2.1)–(2.3) holds in region 2. No generality is lost if we assume that $c_1 > c_2$.

For time $t < 0$ a plane horizontally polarized shear wave of the general form

$$w_1^i(x', y', t) = A_1^i H(c_1 t + x' \cos\alpha - y' \sin\alpha) \int_0^{c_1 t + x' \cos\alpha - y' \sin\alpha} G(u)\,du, \tag{2.4}$$

where $H(\ )$ is the Heaviside step function and $0 < \alpha \leq \pi/2$ impinges upon the bonded interface and thus gives rise to a system of plane reflected and transmitted waves, as shown in Fig. 1. These reflected and transmitted waves are defined by

$$w_1^r(x', y', t) = A_1^r H(c_1 t + x' \cos\alpha + y' \sin\alpha) \int_0^{c_1 t + x' \cos\alpha + y' \sin\alpha} G(u)\,du \tag{2.5}$$

$$w_2^t(x', y', t) = A_2^t H(mc_1 t + x' \cos\beta - y' \sin\beta) \int_0^{c_1 t + (x'/m) \cos\beta - (y'/m) \sin\beta} G(u)\,du, \tag{2.6}$$

respectively, where

$$A_1^r = \frac{km \sin\alpha - \sin\beta}{km \sin\alpha + \sin\beta} A_1^i \tag{2.7}$$

$$A_2^t = \frac{2km \sin\alpha}{km \sin\alpha + \sin\beta} A_1^i \tag{2.8}$$

$$\beta = \cos^{-1}(m \cos\alpha) \tag{2.9}$$

$$k = \mu_1/\mu_2, \qquad m = c_2/c_1 < 1. \tag{2.10a, b}$$

At time $t = 0$, the system of plane waves strikes the tip of the interface region without bond (the interface crack), thus giving rise to a system of diffracted cylindrical shear waves and wedge-like head waves. The pattern of wavefronts for $t > 0$ due to these diffracted and plane waves is shown in Fig. 2. In addition, it is assumed that at the instant the system of plane waves strikes the crack tip, although the interface bond does not rupture, the interface stress immediately ahead of the crack tip reaches the yield value σ. Subsequently this zone of yielding extends along the interface in the positive x'-direction with a constant velocity v where $v < c_2 < c_1$. This extending yield zone is also shown in Fig. 2.

For $t > 0$, the boundary conditions can then be written as

$$y' = 0, -\infty < x' < 0 : \mu_1 \frac{\partial w_1}{\partial y'} = \mu_2 \frac{\partial w_2}{\partial y'} = 0 \tag{2.11}$$

$$y' = 0, 0 \leq x' \leq vt : \mu_1 \frac{\partial w_1}{\partial y'} = \mu_2 \frac{\partial w_2}{\partial y'} = \sigma, \tag{2.12}$$

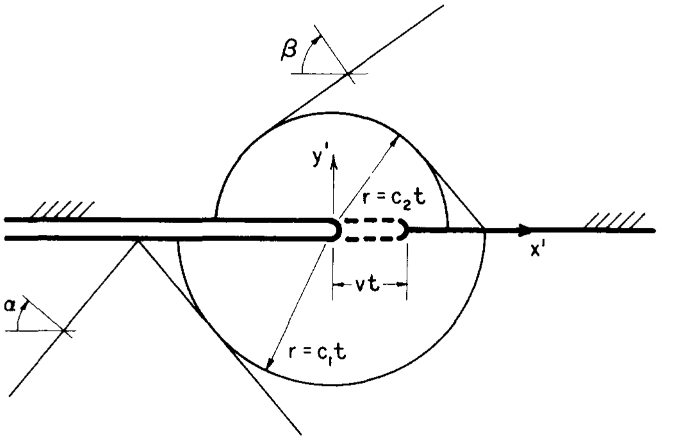

FIG. 2. Pattern of wavefronts after the interface flaw has been struck.

while the displacement and the stress are continuous for $x \geq vt$, i.e.

$$y' = 0, \qquad vt \leq x' < \infty : w_1 - w_2 = 0 \tag{2.13}$$

$$\mu_1 \frac{\partial w_1}{\partial y'} - \mu_2 \frac{\partial w_2}{\partial y'} = 0. \tag{2.14}$$

Furthermore, because the interface bonding is assumed to be rigid-perfectly plastic in nature, the magnitude of the interface stress should nowhere be larger than the yield value σ.

To actually solve the diffraction problem, it is convenient to define the scattered displacements w_1^s and w_2^s by

$$w_1 = w_1^i + w_1^r + w_1^s \tag{2.15}$$

$$w_2 = w_2^t + w_2^s. \tag{2.16}$$

The left-hand sides of (2.15) and (2.16) represent all motion in the two half-spaces. Therefore, the scattered displacements comprise the effect of the interface crack on the system of plane waves w_1^i, w_1^r and w_2^t. Since the scattered displacements also satisfy wave equations of the type given in (2.1) and w_1^i, w_1^r and w_2^t are known, it is possible to recast the problem completely in terms of these scattered displacements. The initial conditions on w_1^s and w_2^s are

$$t = 0 : w_1^s = \dot{w}_1^s = w_2^s = \dot{w}_2^s \equiv 0. \tag{2.17}$$

Similarly, the boundary conditions for $t > 0$ can be obtained from (2.11)–(2.16) as

$y' = 0, -\infty < x' \leq vt$:

$$\mu_1 \frac{\partial w_1^s}{\partial y'} = \mu_2 \frac{\partial w_2^s}{\partial y'} = \sigma H(x') + \frac{\mu_2 \sin \beta}{m} A_2^t G(c_1 t + x' \cos \alpha) H(c_1 t + x' \cos \alpha) \tag{2.18}$$

$$y' = 0, vt \leq x' < \infty : w_1^s - w_2^s = 0 \tag{2.19}$$

$$\mu_1 \frac{\partial w_1^s}{\partial y'} - \mu_2 \frac{\partial w_2^s}{\partial y'} = 0. \tag{2.20}$$

Inspection of (2.17)–(2.20) shows that the scattered problem is a special case of the more general problem of a partially loaded semi-infinite flaw extending uniformly along the interface. In the next sections we proceed to state and then solve this mathematical problem.

3. PROPAGATION OF A LOADED INTERFACE FLAW

Let the two half-spaces described at the outset of the previous section be completely undisturbed for $t < 0$. Subsequent to $t = 0$, let the interface flaw extend in the positive x'-direction with a constant velocity v, where $v < c_2 < c_1$. Furthermore, let the surfaces of the flaw be acted upon by a given shear stress distribution which travels in the negative x'-direction with a given velocity c and covers the region $-ct < x' < vt$. This stress distribution is defined by

$$y = 0, -\infty < x' \le vt: \mu_1 \frac{\partial w_1}{\partial y'} = \mu_2 \frac{\partial w_2}{\partial y'} = f(t + x'/c)H(t + x'/c), \tag{3.1}$$

where $w_1(x', y', t)$ and $w_2(x', y', t)$ are the displacements in the z'-direction for $y' \le 0$ and $y' \ge 0$, respectively.

To solve this mathematical problem, it is convenient to work in a coordinate system whose origin is fixed to the tip of the moving interface flaw. Thus, as shown in Fig. 3, we introduce the following coordinate transformation:

$$\tau = c_1 t, \qquad x = x' - n\tau, \qquad y = y', \qquad z = z', \tag{3.2a, b, c, d}$$

where

$$n = v/c_1 < m < 1. \tag{3.3}$$

In terms of these moving coordinates, the governing displacement equations of motion for the medium of region 1 ($y \le 0$) can be obtained by substituting (3.2) into the wave equation (2.1). The result is

$$(1 - n^2)\frac{\partial^2 w_1}{\partial x^2} + \frac{\partial^2 w_1}{\partial y^2} = \frac{\partial^2 w_1}{\partial \tau^2} - 2n\frac{\partial^2 w_1}{\partial x \partial \tau}. \tag{3.4}$$

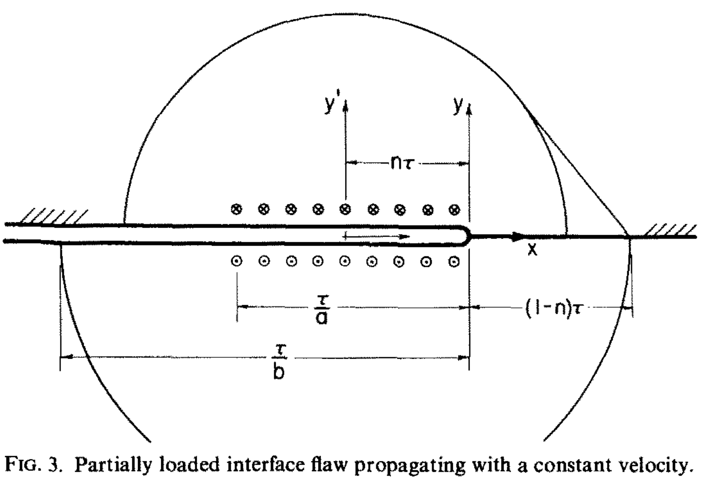

FIG. 3. Partially loaded interface flaw propagating with a constant velocity.

From (2.3) and (3.2) the shear stresses in region 1 become

$$(\tau_{yz})_1 = \mu_1 \frac{\partial w_1}{\partial y}, \qquad (\tau_{xz})_1 = \mu_1 \frac{\partial w_1}{\partial x}, \tag{3.5a, b}$$

while the particle velocity assumes the form

$$\frac{\dot{w}_1}{c_1} = \frac{\partial w_1}{\partial \tau} - n\frac{\partial w_1}{\partial x}. \tag{3.6}$$

Analogously, we obtain for region 2 ($y \geq 0$):

$$\left(1-\frac{n^2}{m^2}\right)\frac{\partial^2 w_2}{\partial x^2} + \frac{\partial^2 w_2}{\partial y^2} = \frac{1}{m^2}\left(\frac{\partial^2 w_2}{\partial \tau^2} - 2n\frac{\partial^2 w_2}{\partial x \partial \tau}\right) \tag{3.7}$$

and

$$(\tau_{yz})_2 = \mu_2 \frac{\partial w_2}{\partial y}, \qquad (\tau_{xz})_2 = \mu_2 \frac{\partial w_2}{\partial x}, \qquad \frac{\dot{w}_2}{c_1} = \frac{\partial w_2}{\partial \tau} - n\frac{\partial w_2}{\partial x}. \tag{3.8a, b, c}$$

Referring to Fig. 3 and equation (3.1) the interface conditions in the system of moving coordinates can be written as

$$y = 0, x < 0: w_1 - w_2 = \varphi_-(x, \tau)H(\tau + bx) \tag{3.9}$$

$$\mu_1 \frac{\partial w_1}{\partial y} = \mu_2 \frac{\partial w_2}{\partial y} = f(\tau + ax)H(\tau + ax) \tag{3.10}$$

$$y = 0, x \geq 0: w_1 - w_2 = 0 \tag{3.11}$$

$$\mu_1 \frac{\partial w_1}{\partial y} = \mu_2 \frac{\partial w_2}{\partial y} = \psi_+(x, \tau)H\left(\tau - \frac{x}{1-n}\right), \tag{3.12}$$

where

$$a = \frac{c_1}{c+v}, \qquad b = \min\left(a, \frac{1}{1+n}\right). \tag{3.13a, b}$$

In (3.9) and (3.12), the functions φ_- and ψ_+ are, respectively, the unknown displacement discontinuity behind the tip of the flaw and the unknown interface stress distribution ahead of the tip. These unknown functions have been introduced so that sets of conditions for both the displacements and their derivatives can be stated everywhere on $y = 0$, $|x| < \infty$. The Heaviside functions multiplying φ_- and ψ_+ illustrate the wave propagation character of w_1 and w_2. Finally, it can be checked that the initial conditions on w_1 and w_2 can be written as

$$\tau = 0: w_1 = \frac{\partial w_1}{\partial \tau} = w_2 = \frac{\partial w_2}{\partial \tau} \equiv 0. \tag{3.14}$$

To solve the set of equations (3.4)–(3.14), Laplace transforms are introduced, first over τ and subsequently over x. The one-sided Laplace transform over the time-related variable τ is defined as

$$\bar{g}(x, y, s) = \int_0^\infty g(x, y, \tau)\, e^{-s\tau}\, d\tau, \tag{3.15}$$

where s is a positive real number large enough to insure convergence of the integral. It is convenient to define the two-sided Laplace transform over the spatial variable x as

$$\bar{g}^*(\lambda, y, s) = \int_{-\infty}^{\infty} \bar{g}(x, y, s)\, e^{-s\lambda x}\, dx, \tag{3.16}$$

where λ is, in general, complex. The interval of convergence for this transform is determined by the asymptotic behavior of $\bar{g}$ as $x \to \pm\infty$.

Performing the operations indicated by (3.15) and (3.16) on (3.4), (3.7) and (3.9)–(3.12) while making use of (3.14) yields the following set of transformed equations:

$$y \leq 0: \frac{d^2\bar{w}_1^*}{dy^2} + s^2[\lambda^2 - (\lambda n - 1)^2]\bar{w}_1^* = 0 \tag{3.17}$$

$$y \geq 0: \frac{d^2\bar{w}_2^*}{dy^2} + s^2\left[\lambda^2 - \frac{(\lambda n - 1)^2}{m^2}\right]\bar{w}_2^* = 0 \tag{3.18}$$

$$y = 0: \bar{w}_2^* - \bar{w}_1^* = \bar{\varphi}_-^*(\lambda, s) \tag{3.19}$$

$$\mu_1 \frac{d\bar{w}_1^*}{dy} = \mu_2 \frac{d\bar{w}_2^*}{dy} = \bar{\psi}_+^*(\lambda, s) + \frac{\bar{f}(s)}{s(a-\lambda)}, \tag{3.20}$$

where $\bar{f}(s)$ is the one-sided Laplace transforms of $f(\tau)$.

The right-hand sides of (3.19) and (3.20) represent the twice-transformed right-hand sides of (3.9)–(3.12). It can be checked that the one-sided Laplace transforms over τ of the right-hand sides of (3.9) and (3.10) vanish identically for $x > 0$ and behave as e^{sbx} and e^{sax}, respectively, as $x \to -\infty$. Similarly, the one-sided transforms of the right-hand side of (3.12) vanish for $x < 0$ and behave as $e^{-sx/(1-n)}$ as $x \to \infty$. Therefore, since s is real and positive, the functions $\bar{\varphi}_-^*$ and $1/(a-\lambda)$ are valid as transforms only in that part of the complex λ-plane defined by, respectively, Re $\lambda < b$ and Re $\lambda < a$. Analogously, $\bar{\psi}_+^*$ exists as a transform for Re $\lambda > -1/(1-n)$. Furthermore, because w_1 and w_2 vanish identically for $y = 0$ outside the range $-\tau/b < x < (1-n)\tau$, their transforms over x and τ can be expected to exist in that part of the complex λ-plane defined by $-1/(1-n) < \text{Re}\,\lambda < b$. From the foregoing considerations it can be concluded that the vertical strip in the complex λ-plane defined by $-1/(1-n) < \text{Re}\,\lambda < b$ comprises a domain of analyticity common to all the transformed functions.

Returning to the differential equations (3.17) and (3.18), we obtain the following bounded solutions:

$$y \leq 0: \bar{w}_1^*(\lambda, y, s) = B_1(\lambda, s)\, e^{s(1-n^2)^{\frac{1}{2}}\gamma_1(\lambda)y}, \qquad \text{Re}\,\gamma_1 \geq 0 \tag{3.21}$$

$$y \geq 0: \bar{w}_2^*(\lambda, y, s) = B_2(\lambda, s)\, e^{-s(1-n^2/m^2)^{\frac{1}{2}}\gamma_2(\lambda)y}, \qquad \text{Re}\,\gamma_2 \geq 0, \tag{3.22}$$

where

$$\gamma_1(\lambda) = \left(\frac{1}{1-n} + \lambda\right)^{\frac{1}{2}}\left(\frac{1}{1+n} - \lambda\right)^{\frac{1}{2}} \tag{3.23}$$

$$\gamma_2(\lambda) = \left(\frac{1}{m-n} + \lambda\right)^{\frac{1}{2}}\left(\frac{1}{m+n.} - \lambda\right)^{\frac{1}{2}}. \tag{3.24}$$

To insure that Re $\gamma_1 \geq 0$ and Re $\gamma_2 \geq 0$ everywhere in the cut complex λ-plane, appropriate Riemann sheets are chosen for γ_1 and γ_2. In (3.21) and (3.22), $B_1(\lambda, s)$ and $B_2(\lambda, s)$ are unknown functions which are analytic in the strip $-1/(1-n) < \text{Re}\,\lambda < b$.

4. SOLUTIONS BY MEANS OF THE WIENER–HOPF TECHNIQUE

From (3.19) and (3.20) we can obtain the following equations:

$$y = 0: \bar{w}_1^* - \bar{w}_2^* = \bar{\varphi}_-^*(\lambda, s) \tag{4.1}$$

$$\mu_1 \frac{d\bar{w}_1^*}{dy} - \mu_2 \frac{d\bar{w}_2^*}{dy} = 0. \tag{4.2}$$

Then, substituting (3.21) and (3.22) into (4.1) and (4.2) enables us to eliminate B_1 and B_2 as follows:

$$B_1(\lambda, s) = \mu_2 \frac{(1-n^2/m^2)^{\frac{1}{2}}\gamma_2(\lambda)\bar{\varphi}_-^*(\lambda, s)}{\mu_1(1-n^2)^{\frac{1}{2}}\gamma_1(\lambda)+\mu_2(1-n^2/m^2)^{\frac{1}{2}}\gamma_2(\lambda)} \tag{4.3}$$

$$B_2(\lambda, s) = -\mu_1 \frac{(1-n^2)^{\frac{1}{2}}\gamma_1(\lambda)\bar{\varphi}_-^*(\lambda, s)}{\mu_1(1-n^2)^{\frac{1}{2}}\gamma_1(\lambda)+\mu_2(1-n^2/m^2)^{\frac{1}{2}}\gamma_2(\lambda)}, \tag{4.4}$$

whereupon equation (3.20) can be made to yield the following equation of the Wiener–Hopf type:

$$\mu_1\mu_2 \frac{(1-n^2)^{\frac{1}{2}}(1-n^2/m^2)^{\frac{1}{2}}\gamma_1(\lambda)\gamma_2(\lambda)s\bar{\varphi}_-^*(\lambda, s)}{\mu_1(1-n^2)^{\frac{1}{2}}\gamma_1(\lambda)+\mu_2(1-n^2/m^2)^{\frac{1}{2}}\gamma_2(\lambda)} = \bar{\psi}_+^*(\lambda, s) + \frac{\bar{f}(s)}{s(a-\lambda)}. \tag{4.5}$$

Upon examining the left-hand side of (4.5), it is noted that

$$\lim_{|\lambda|\to\infty} \frac{\mu_1(1-n^2)^{\frac{1}{2}}\gamma_1(\lambda)+\mu_2(1-n^2/m^2)^{\frac{1}{2}}\gamma_2(\lambda)}{\mu_2(1-n^2/m^2)^{\frac{1}{2}}\gamma_2(\lambda)} = 1 + km\left(\frac{1-n^2}{m^2-n^2}\right)^{\frac{1}{2}}. \tag{4.6}$$

It is therefore convenient to define the related function $F(\lambda)$, where

$$F(\lambda) = \frac{\mu_1(1-n^2)^{\frac{1}{2}}\gamma_1(\gamma)+\mu_2(1-n^2/m^2)^{\frac{1}{2}}\gamma_2(\lambda)}{\kappa\mu_2(1-n^2/m^2)^{\frac{1}{2}}\gamma_2(\lambda)} \tag{4.7}$$

$$\kappa = 1 + km\left(\frac{1-n^2}{m^2-n^2}\right)^{\frac{1}{2}}. \tag{4.8}$$

It can be checked that $F(\lambda)$ is analytic in the strip $-1/(1-n) < \text{Re}\,\lambda < 1/(1+n)$ and moreover, from (4.6)–(4.8) it has the property that

$$\lim_{|\lambda|\to\infty} \ln F(\lambda) = 0. \tag{4.9}$$

Then, from analytic function theory it is known that $F(\lambda)$ can be factored into a product of functions which are analytic in overlapping half-planes, the overlap region being the strip $-1/(1-n) < \text{Re}\,\lambda < 1/(1+n)$. Performing this factorization leads to the result

$$F(\lambda) = F_+(\lambda)F_-(\lambda), \tag{4.10}$$

where, from Noble [3], we have that

$$\ln F_+(\lambda) = \frac{-1}{2\pi i}\int_{c-i\infty}^{c+i\infty} \frac{\ln F(z)\,\mathrm{d}z}{z-\lambda} \tag{4.11}$$

$$\ln F_-(\lambda) = \frac{+1}{2\pi i}\int_{d-i\infty}^{d+i\infty} \frac{\ln F(z)\,\mathrm{d}z}{z-\lambda}. \tag{4.12}$$

In (4.11) and (4.12), c and d are any real numbers such that

$$-1/(1-n) < c < \operatorname{Re}\lambda < d < 1/(1+n). \tag{4.13}$$

By using Cauchy's theorem, the right-hand sides of (4.11) and (4.12) can be transformed into integrals about, respectively, the left-hand and right-hand branch cuts of $\ln F(z)$ in the complex z-plane. This leads to the following expressions for $F_+(\lambda)$ and $F_-(\lambda)$:

$$F_\pm(\lambda) = \exp\left\{\mp\frac{1}{\pi}\int_{1/(1\mp n)}^{1/(m\mp n)} \tan^{-1}\left[\frac{km[(1-n)z\mp 1]^{\frac{1}{2}}[(1+n)z\pm 1]^{\frac{1}{2}}}{[1\pm(m+n)z]^{\frac{1}{2}}[1\mp(m-n)z]^{\frac{1}{2}}}\right]\frac{\mathrm{d}z}{z\pm\lambda}\right\}. \tag{4.14}$$

It can be checked that, indeed, F_+ is analytic for $\operatorname{Re}\lambda > -1/(1-n)$ while F_- is analytic for $\operatorname{Re}\lambda < 1/(1+n)$. It is now possible to rewrite (4.5) as follows:

$$\mu_1\frac{(1-n^2)^{\frac{1}{2}}\gamma_1^-(\lambda)s\bar{\varphi}_-^*(\lambda, s)}{\kappa F_-(\lambda)} = \frac{F_+(\lambda)\bar{\psi}_+^*(\lambda, s)}{\gamma_{1+}(\lambda)} + \frac{F_+(\lambda)\bar{f}(s)}{\gamma_{1+}(\lambda)s(a-\lambda)}, \tag{4.15}$$

where

$$\gamma_{1+}(\lambda) = \left(\frac{1}{1-n}+\lambda\right)^{\frac{1}{2}}, \qquad \gamma_{1-}(\lambda) = \left(\frac{1}{1+n}-\lambda\right)^{\frac{1}{2}}. \tag{4.16a, b}$$

Upon studying the right-hand side of (4.15), we notice that the function $F_+/\gamma_{1+}(a-\lambda)$ is analytic in the strip $-1/(1-n) < \operatorname{Re}\lambda < a$ and that, moreover,

$$\frac{F_+(\lambda)}{\gamma_{1+}(\lambda)(a-\lambda)} \sim \mathrm{O}(|\lambda|^{-\frac{3}{2}}) \text{ as } |\lambda| \to \infty. \tag{4.17}$$

Then, once again from analytic function theory, it is known that this function can be split into the sum of two functions which are analytic in overlapping half-planes, the overlap region being the strip $-1/(1-n) < \operatorname{Re}\lambda < a$. Performing this splitting by inspection yields

$$\frac{F_+(\lambda)}{\gamma_{1+}(\lambda)(a-\lambda)} = G_+(\lambda)+G_-(\lambda), \tag{4.18}$$

where

$$G_-(\lambda) = \frac{F_+(a)}{\gamma_{1+}(a)(a-\lambda)} \tag{4.19}$$

$$G_+(\lambda) = \left[\frac{F_+(\lambda)}{\gamma_{1+}(\lambda)} - \frac{F_+(a)}{\gamma_{1+}(a)}\right]\frac{1}{a-\lambda}. \tag{4.20}$$

It can be seen that, indeed, G_+ is analytic for $\operatorname{Re}\lambda > -1/(1-n)$ while G_- is analytic for $\operatorname{Re}\lambda < a$. Using these results, we can now rearrange (4.15) to yield

$$\mu_1\frac{(1-n^2)^{\frac{1}{2}}\gamma_{1-}(\lambda)s\bar{\varphi}_-^*(\lambda, s)}{\kappa F_-(\lambda)} - G_-(\lambda)\frac{\bar{f}(s)}{s} = \frac{F_+(\lambda)\bar{\psi}_+^*(\lambda, s)}{\gamma_{1+}(\lambda)} + G_+(\lambda)\frac{\bar{f}(s)}{s}. \tag{4.21}$$

From the above manipulations it is clear that the left-hand and right-hand sides of (4.21) are analytic in, respectively, the overlapping half-planes $\operatorname{Re}\lambda < b$ and $\operatorname{Re}\lambda > -1/(1-n)$. Therefore, by analytic continuation, both sides of (4.21) represent the same entire function, say $E(\lambda, s)$. Now from the standard Abelian theorems for Laplace transforms (see Noble [3]) and using (3.9), (3.11) and (3.19) we obtain

$$\bar{w}_1(0^-, 0, s) - \bar{w}_2(0^-, 0, s) \sim \lim_{|\lambda|\to\infty} s\lambda\bar{\varphi}^*_-(\lambda, s). \tag{4.22}$$

But (3.11) implies that the left-hand side of (4.22) must vanish. Therefore, we have that

$$\bar{\varphi}^*_-(\lambda, s) \sim 0(\lambda^{-1-\varepsilon}), \qquad \varepsilon > 0, \quad \text{as } |\lambda| \to \infty. \tag{4.23}$$

Then, from checking the left-hand side of (4.21) in conjunction with (4.14), (4.16b) and (4.19), we see that

$$\lim_{|\lambda|\to\infty} E(\lambda, s) = 0. \tag{4.24}$$

But from Liouville's theorem concerning entire functions, (4.24) implies that $E \equiv 0$, whereupon (4.21) can be made to yield the results

$$\bar{\varphi}^*_-(\lambda, s) = \frac{\kappa F_-(\lambda) G_-(\lambda) \bar{f}(s)}{\mu_1(1-n^2)^{\frac{1}{2}} \gamma_{1-}(\lambda) s^2} \tag{4.25}$$

$$\bar{\psi}^*_+(\lambda, s) = \frac{-\gamma_{1+}(\lambda) G_+(\lambda) \bar{f}(s)}{s F_+(\lambda)}. \tag{4.26}$$

Then, substituting (4.25) into (4.3) and (4.4) we obtain

$$B_1(\lambda, s) = \frac{G_-(\lambda)\bar{f}(s)}{\mu_1(1-n^2)^{\frac{1}{2}}\gamma_{1-}(\lambda)F_+(\lambda)s^2} \tag{4.27}$$

$$B_2(\lambda, s) = \frac{-\gamma_{1+}(\lambda)G_-(\lambda)\bar{f}(s)}{\mu_2(1-n^2/m^2)^{\frac{1}{2}}\gamma_2(\lambda)F_+(\lambda)s^2}, \tag{4.28}$$

whereupon (3.21) and (3.22) can be made to yield

$$y \le 0: \bar{w}^*_1(\lambda, y, s) = \frac{G_-(\lambda)\bar{f}(s)e^{s(1-n^2)^{\frac{1}{2}}\gamma_1(\lambda)y}}{\mu_1(1-n^2)^{\frac{1}{2}}\gamma_{1-}(\lambda)F_+(\lambda)s^2} \tag{4.29}$$

$$y \ge 0: \bar{w}^*_2(\lambda, y, s) = \frac{-\gamma_{1+}(\lambda)G_-(\lambda)\bar{f}(s)e^{-s(1-n^2/m^2)^{\frac{1}{2}}\gamma_2(\lambda)y}}{\mu_2(1-n^2/m^2)^{\frac{1}{2}}\gamma_2(\lambda)F_+(\lambda)s^2}. \tag{4.30}$$

With the above expressions at hand, the mathematical problem stated in the previous section is essentially solved. Since, in later sections, we will be interested in the interface stress ahead of the extending tip of the flaw ($x > 0$) we list for future reference

$$\bar{\tau}^*_{yz}(\lambda, 0, s) = \mu_1 \frac{d\bar{w}^*_1(\lambda, 0, s)}{dy} = \mu_2 \frac{d\bar{w}^*_2(\lambda, 0, s)}{dy}$$

$$= \frac{\gamma_{1+}(\lambda)G_-(\lambda)\bar{f}(s)}{sF_+(\lambda)}. \tag{4.31}$$

As a closing comment to this section it is noted that by means of the substitution $z = 1/(\zeta \mp n)$, equation (4.14) can be expressed in the form

$$F_{\pm}(\lambda) = \exp\left\{\mp\frac{1}{\pi}\int_m^1 \tan^{-1}\left[km\left(\frac{1-\zeta^2}{\zeta^2-m^2}\right)^{\frac{1}{2}}\right]\frac{\mathrm{d}\zeta}{(\zeta\mp n)[1\pm\lambda(\zeta\mp n)]}\right\}, \tag{4.32}$$

which is more convenient for numerical computations.

5. INVERSIONS OF THE TRANSFORMS

To invert the double transforms of the interface stress, de Hoop's modification of Cagniard's method [4] is used. In this procedure, the path of integration of the inversion integral for the two-sided Laplace transform over x is shifted to another path in the complex λ-plane, called a Cagniard contour, such that the resulting integral is recognizable as an explicit one-sided Laplace transform over τ.

The inverse of the bilateral Laplace transform over x is defined by

$$g(x) = \frac{s}{2\pi i}\int_{\lambda_0 - i\infty}^{\lambda_0 + i\infty} g^*(s\lambda)\,\mathrm{e}^{s\lambda x}\,\mathrm{d}\lambda, \tag{5.1}$$

where λ_0 must lie in the range of analyticity of the transform g^*. Thus, the Laplace transform of the interface stress ahead of the crack tip may be obtained in a formal manner from (4.31) as

$$\bar{\tau}_{yz}(x,0,s) = \frac{1}{2\pi i}\int_{\lambda_0 - i\infty}^{\lambda_0 + i\infty} \bar{f}(s)\frac{\gamma_{1+}(\lambda)G_-(\lambda)\,\mathrm{e}^{s\lambda x}}{F_+(\lambda)}\,\mathrm{d}\lambda, \qquad x > 0, \tag{5.2}$$

where

$$-1/(1-n) < \lambda_0 < b. \tag{5.3}$$

Upon examining the integrand of (5.2), it can be checked that $\gamma_{1+}G_-/F_+ \sim 0(|\lambda|^{-\frac{1}{2}})$ as $|\lambda| \to \infty$. Then, because s and x are both real and strictly positive, the integrand of (5.2) vanishes exponentially for Re $\lambda < 0$ as $|\lambda| \to \infty$. Moreover, because $a > 0$, $\gamma_{1+}G_-/F_+$ has no poles in the complex λ-plane for Re $\lambda < 0$. Therefore, by Cauchy's theorem, the integral shown in (5.2) may be replaced by an integration about the branch cut of the integrand in the left-hand half of the complex λ-plane. Then, it can be shown that (5.2) takes the form

$$[\bar{\tau}_{yz}(x,0,s)]_{1,2} = -\frac{1}{\pi}\int_{x/(m-n)}^{\infty} \bar{f}(s)\frac{\gamma_{1i+}(-\xi/x)G_-(-\xi/x)\,\mathrm{e}^{-s\xi}}{xF_+(-\xi/x)}\,\mathrm{d}\xi$$
$$-\frac{\kappa}{\pi}\int_{x/(1-n)}^{x/(m-n)} \bar{f}(s)\frac{\gamma_{1i+}(-\xi/x)F_-(-\xi/x)G_-(-\xi/x)\,\mathrm{e}^{-s\xi}}{1-k^2m^2\left(\dfrac{1-n^2}{m^2-n^2}\right)\dfrac{\gamma_1^2(-\xi/x)}{\gamma_2^2(-\xi/x)}}\frac{\mathrm{d}\xi}{x},$$
$$x > 0, \tag{5.6}$$

where γ_{1i+} is the imaginary part of γ_{1+},

$$\gamma_{1i+}(-\xi/x) = \left(\frac{\xi}{x} - \frac{1}{1-n}\right)^{\frac{1}{2}}. \tag{5.7}$$

The inverse Laplace transform over the time-related variable τ of (5.6) can be obtained by inspection. Then, making use of (4.19) and introducing the change of variable $\xi = xu$ we obtain the following expression for the interface stress ahead of the crack tip:

$$[\tau_{yz}(x,0,\tau)]_{1,2} = -\frac{F_+(a)}{\pi\gamma_{1+}(a)}\int_{1/(m-n)}^{\infty}\frac{\gamma_{1i+}(-u)f(\tau-xu)H(\tau-xu)}{F_+(-u)(a+u)}\,\mathrm{d}u$$
$$-\frac{\kappa F_+(a)}{\pi\gamma_{1+}(a)}\int_{1/(1-n)}^{1/(m-n)}\frac{\gamma_{1i+}(-u)F_-(-u)f(\tau-xu)H(\tau-xu)}{\left[1-k^2m^2\left(\frac{1-n^2}{m^2-n^2}\right)\frac{\gamma_1^2(-u)}{\gamma_2^2(-u)}\right](a+u)}\,\mathrm{d}u, \qquad x>0. \tag{5.8}$$

For small positive values of x we have

$$\tau_{yz}(x,0,\tau) \sim -\frac{F_+(a)}{\pi\gamma_{1+}(a)}\frac{1}{x^{\frac{1}{2}}}\int_0^{\tau}\frac{f(\tau-\xi)}{\xi^{\frac{1}{2}}}\,\mathrm{d}\xi + 0(x^{\frac{1}{2}}). \tag{5.9}$$

In the next section these solutions are applied to the problem of fracture mechanics defined in Section 2.

6. FRACTURE MECHANICS ASPECTS

Upon rewriting the interface condition (2.18) in terms of the moving coordinates defined by (3.2) and comparing it to the corresponding condition for the mathematical problem (3.10), it is noted that the solution for the boundary conditions (2.18)–(2.20) can be obtained as the superposition of the solutions to two separate problems of the type solved in Sections 3–5. For the first of these, we have

$$a = \frac{1}{n}, \qquad b = \frac{1}{1+n}, \qquad f(\tau+ax) = \sigma H\left(\tau+\frac{x}{n}\right), \tag{6.1a, b, c}$$

while for the second

$$a = b = \frac{\cos\alpha}{1+n\cos\alpha}, \qquad f(\tau+ax) = \mu_2\frac{\sin\beta}{m}A_2'G\left(\tau+\frac{x\cos\alpha}{1+n\cos\alpha}\right). \tag{6.2a, b}$$

The solution to the diffraction problem defined in Section 2 can then be obtained by superimposing the system of plane waves given by (2.4)–(2.6).

It should be noted that the solutions thus obtained contain the extension velocity of the yield zone as a parameter. This velocity, although assumed to be subsonic, is otherwise completely unspecified. To determine this velocity, we require that the mathematical solutions satisfy yet another condition, which is obtained by an examination of the fracture mechanics aspects of the problem. From (5.9) it can be seen that the interface stress exhibits a square-root singularity at the leading edge of the yield zone, thus seeming to violate the assumption of a rigid-perfectly plastic interface bond. Following the work of Dugdale [5] and Barenblatt [6], we will, however, append the condition that the components of the stress distributions are related such that the square-root singularities in the interface stress cancel out at the leading edge of the yield zone. Then, from (5.9), (6.1) and (6.2) we see that we must have

$$G(u) = H(u), \tag{6.3}$$

and therefore

$$\frac{\sigma F_+\left(\frac{1}{n}\right)}{\gamma_{1+}\left(\frac{1}{n}\right)} = -\mu_2\frac{\sin\beta}{m}A_2^t\frac{F_+\left(\frac{\cos\alpha}{1+n\cos\alpha}\right)}{\gamma_{1+}\left(\frac{\cos\alpha}{1+n\cos\alpha}\right)}. \tag{6.4}$$

Condition (6.3) states that the assumed constant velocity of the leading edge of the yield zone can be attained only if the incident plane wave is a step-stress pulse. From (2.4) it can be checked that the actual magnitude of this pulse τ_α is givên by

$$\tau_\alpha = -\mu_1 A_1^i, \tag{6.5}$$

whereupon, making use of (2.8), (2.9) and (4.32), equation (6.4) can be rearranged to yield

$$\frac{\tau_\alpha}{\sigma} = \frac{km\sin\alpha+\sin\beta}{2\sin\beta(1-\cos\alpha)^{\frac{1}{2}}}\left(\frac{n}{1+n\cos\alpha}\right)^{\frac{1}{2}}M(\cos\alpha), \tag{6.6}$$

where $M(u)$ is obtained, after some manipulation, and by employing equation (4.32), as

$$M(u) = \exp\left\{\frac{1}{\pi}\int_m^1\tan^{-1}\left[km\left(\frac{1-z^2}{z^2-m^2}\right)^{\frac{1}{2}}\right]\frac{dz}{z(1+zu)}\right\}. \tag{6.7}$$

The expression (6.6) can now be solved for the normalized yield zone velocity $n = v/c_1$ as

$$\frac{v}{c_1} = \frac{\left(\frac{\tau_\alpha}{\sigma}\right)^2}{\left[\frac{km\sin\alpha+\sin(\beta)M(\cos\alpha)}{2\sin\beta(1-\cos\alpha)^{\frac{1}{2}}}\right]^2-\left(\frac{\tau_\alpha}{\sigma}\right)^2\cos\alpha} \tag{6.8}$$

Thus, the condition for the removal of the stress singularities gives the relation needed to determine the yield zone extension velocity in terms of the incident stress τ_α. For various values of τ_α/σ, k and m, the value of v/c_1 is plotted versus the value of the angle of incidence α in Fig. 4.

With the results of the previous section thus interpreted, the superposition procedure outlined above gives complete solutions to the originally stated fracture mechanics problem. After some manipulation the interface stress ahead of the uniformly extending yield zone can be expressed in terms of the fixed coordinates as

$$\begin{aligned}\tau_{yz}(x',0,\tau) &= \frac{\sigma\sqrt{n}}{\pi}\int_n^m\left(\frac{1-u}{u-n}\right)^{\frac{1}{2}}\frac{M(-1/u)H(u-x'/\tau)}{u(1+u\cos\alpha)}du\\ &\quad+[1+(1+k)k]\frac{\sigma\sqrt{n}}{\pi}\int_m^1\left(\frac{1-u}{u-n}\right)^{\frac{1}{2}}\frac{(u^2-m^2)M(1/u)H(u-x'/\tau)}{[u^2-m^2+k^2m^2(1-u^2)](1+u\cos\alpha)}\frac{du}{u}\\ &\quad-\frac{2\sin\alpha\sin\beta}{km\sin\alpha+\sin\beta}\tau_\alpha, \qquad x' > n\tau.\end{aligned} \tag{6.9}$$

Upon concluding this section it should again be noted that we have obtained basically a short-time solution. It is to be expected that at some time $t_{cr} > 0$ the relative displacement between the two sides of the yield zone near the tip of the original flaw ($x' = 0$ or $x = -c_1 t_{cr}$)

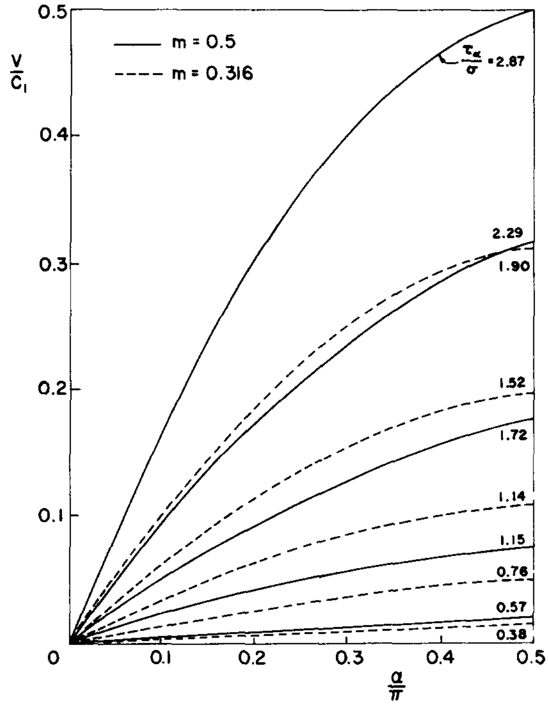

FIG. 4. Velocity of the leading edge of the zone of interface yielding as a function of α, for $\mu_1/\mu_2 = 10$ and for various values of τ_α/σ.

becomes so great that the bond between the half-spaces there actually ruptures. If we assume that the magnitude of this critical relative displacement for rupture is a known property of the bond, say δw_{cr}, then we can compute

$$t_{cr} = \delta w_{cr}/c_1|K(\alpha, n)|, \tag{6.10}$$

where $K(\alpha, n)$ can be computed as

$$K(\alpha, n) = \frac{\sigma\sqrt{n}}{\pi\mu_1}\int_0^1 \frac{M(1/u)\,du}{(n+u)^{\frac{1}{2}}(1-u)^{\frac{1}{2}}(1-u\cos\alpha)} + \frac{\sigma m\sqrt{n}}{\pi\mu_2}\int_0^m \frac{M(1/u)(1+u)^{\frac{1}{2}}\,du}{(n+u)^{\frac{1}{2}}(m^2-u^2)^{\frac{1}{2}}(1-u\cos\alpha)} + \frac{2\tau_\alpha}{\mu_1}. \tag{6.11}$$

7. CONCLUDING REMARKS

In this paper we have examined the extension of a flaw along the bonded interface of two elastic solids of different elastic constants and mass densities. The extension is caused by stress concentrations that are generated when a system of transient horizontally polarized shear waves strikes the tip of the flaw. It is assumed that rupture of the adhesive bond is preceded by yielding of the adhesive, but not of the adjoining elastic materials. Thus, as the system of waves strikes the flaw a region of yielding is assumed to develop at the interface. It is assumed that the adhesive behaves as a perfectly plastic material, so that the stress in the zone of interface yielding is uniform and equal to the yield stress. The speed of the leading edge of the zone of yielding is computed from the condition that the interface stress does not exceed the yield stress. For a system of step-stress waves the zone of interface yielding initially extends linearly with time. For various values of the parameters defining the materials and the system of waves the velocity of the leading edge of the zone of yielding is shown in Fig. 4. After a certain amount of yielding has taken place the bond ruptures at the trailing edge of the zone of yielding and additional free surface is produced. Analytic expressions are presented for the time of rupture and for the interface stress ahead of the leading edge of the zone of yielding.

The model that is used in this paper to account for plastic flow in the adhesive bond is analogous to the Dugdale model for the description of ductility effects in a homogeneous material. For a homogeneous material the Dugdale model assumes a narrow zone of yielding in the plane of the crack. At least for static problems there is, however, evidence that the plastic zone in the vicinity of a crack tip in a homogeneous material is a region of some width. On the other hand, for two adhesively joined solids it is not unreasonable to assume that the adhesive has such properties that the stresses in the vicinity of the tip of an interface flaw are released by yielding of the adhesive, without plastic flow of the adjoining materials.

For anti-plane shear the discontinuity in the surface tractions at the trailing edge of the plastic zone produces a logarithmic singularity in the stress τ_{xz}. Conceptually the model can easily be modified to employ a ramp-type distribution of the yield stress which would not give rise to logarithmic singularities. It can then, however, be argued that for the principal purpose of the analysis, which is to determine the locations of the leading edge of the zone of interface yielding, the time of rupture and the interface stress ahead of the leading edge of the yield zone, the difference between a ramp-type distribution and a step-distribution of the yield stress is not significant enough to abandon the analytically much more amenable step-distribution.

Acknowledgment—This work was supported by the U.S. Army Research Office-Durham under Grant No. DA-ARO-D-31-124-71-G155.

REFERENCES

[1] J. D. ACHENBACH, Brittle and ductile extension of a finite crack by a horizontally polarized shear wave. *Int. J. Engng Sci.* **8**, 947 (1970).
[2] J. D. ACHENBACH, Extension of a crack by a shear wave. *Z. angew. Math. Phys.* **21**, 887 (1970).
[3] B. NOBLE, *Methods Based on the Wiener–Hopf Technique.* Pergamon Press (1958).
[4] A. T. DE HOOP, A modification of Cagniard's method for solving seismic pulse problems. *Appl. Sci. Res.* **B8**, 349 (1960).
[5] D. S. DUGDALE, Yielding of steel sheets containing slits. *J. Mech. Phys. Solids* **8**, 100 (1960).
[6] G. I. BARENBLATT, The mathematical theory of equilibrium cracks in brittle fracture. *Adv. appl. Mech.* **7**, 55 (1962).

(*Received* 6 *December* 1971; *revised* 17 *March* 1972)

Абстракт—Работа исследует процесс начала расцепления на поверхности раздела двух упругих твердых тел, обладающих разными упругими постоянными и плотностями массы. Зто расцепление происходит вследствие концентраций напряжений, которые производят, когда система нестационарных горизонтально поляризированных волн сдвига ударяет в вертину трещины поверхности раздела. Предполагается что разрушение связывающего соединения начняется путем течения самого сцепления. Указано, что для системы волн скачкообразных напряжений, зона течения поверхности раздела начально увеличивается линейно в зависимости от времени. Для разных значений параметров, определяющих материалы и системы волн, вычисляется скорость ведущего края зоны течения поверхности раедела. Даются аналитические выражения для времени разрыва и для напряжения на поверхности раздела, для области перед зоной течения.